Molecular Therapy
Oncolytics
Original Article

Oncolytic vaccinia virus induces a novel phenotype of CD8$^+$ effector T cells characterized by high ICOS expression

Midori Yamashita,[1] Mamoru Tasaki,[1] Ryuji Murakami,[1] Yukinori Arai,[1] Takafumi Nakamura,[2] and Shinsuke Nakao[1]

[1]Drug Discovery Research, Astellas Pharma, Inc., 21, Miyukigaoka, Tsukuba 305-8585, Japan; [2]Department of Biomedical Science, Graduate School of Medical Sciences, Tottori University, 86 Nishi-cho, Yonago 683-8503, Japan

Characterization of the intratumoral immune status is important for developing immunotherapies and evaluating their antitumor effectiveness. CD8$^+$ T cells are one of the most important cell types that directly and indirectly contribute to antitumor efficacy by releasing cytolytic molecules and inflammatory cytokines in the tumor microenvironment. Previously, we engineered a tumor-selective oncolytic vaccinia virus that encodes interleukin-7 (IL-7) and IL-12 and demonstrated its usefulness as an agent for *in situ* vaccination against tumors, with data showing that antitumor efficacy was reliant upon CD8$^+$ T cells recruited by viral treatment. Here, we investigated the phenotypic changes in intratumoral CD8$^+$ T cells caused by this oncolytic virus and found increased expression of inducible co-stimulator (ICOS) in PD-1$^-$CD8$^+$ T cells. Unlike previously reported ICOS$^+$CD8$^+$ T cells, a subset of ICOS$^+$PD-1$^-$CD8$^+$ T cells showed effector function characterized by granzyme B expression. ICOS expression was induced by the backbone virus, which did not encode any immune transgenes and was independent of upregulation of the type I interferon pathway. Not only did we identify a novel effector cell subset characterized by ICOS expression, but our findings also shed light on a potential unknown aspect of the mechanism of oncolytic vaccinia virotherapy.

INTRODUCTION

Immune checkpoint blockade targeting programmed cell death-1 (PD-1), programmed cell death-1 ligand-1 (PD-L1), and cytotoxic T lymphocyte antigen 4 (CTLA4) has markedly improved clinical responses in many types of advanced cancer.[1–4] However, the durable benefit is limited to a proportion of patients, likely because of the involvement of multiple immune pathways in the tumor microenvironment.[5,6] To identify an appropriate therapeutic approach, a number of immunotherapies and their combinations have been investigated in clinical and preclinical studies.[7,8] Among these, *in situ* vaccination using tumor-selective oncolytic viruses is a promising candidate.[9] Oncolytic viruses primarily replicate in cancer cells, inducing immunogenic cell death and releasing tumor antigens with damage-associated molecular patterns (DAMPs) and pathogen-associated molecular patterns (PAMPs), resulting in local induction of antitumor immunity.[9] The first-in-class oncolytic virus approved in the United States was talimogene laherparepvec (T-VEC), an engineered herpes simplex virus (HSV) that encodes a gene for granulocyte macrophage colony-stimulating factor (GM-CSF).[10,11] GM-CSF secreted from cancer cells infected with T-VEC is expected to function as an immune adjuvant; likewise, immunomodulatory payloads incorporated into the genome of an oncolytic virus may potentially contribute to further immune status changes in the tumor microenvironment, resulting in an improvement in antitumor efficacy.[12] We previously explored an *in situ* vaccination approach using a tumor-selective oncolytic vaccinia virus carrying immunomodulatory molecules and demonstrated that intratumoral dual expression of interleukin-7 (IL-7) and IL-12 mediated by an oncolytic vaccinia virus dramatically enhanced the antitumor immune response and improved efficacy in several mouse models.[13] IL-7, a crucial molecule for T cell homeostasis, contributes to reconstitution of the intratumoral immune status by increasing the number of tumor-reactive T cells and antagonizing transforming growth factor-β (TGF-β) signaling.[14,15] IL-12 is a well-studied, strong activator of both innate and adaptive immunity through induction of interferon gamma (IFN-γ).[16] The antitumor activity of an oncolytic vaccinia virus carrying human IL-7 and murine IL-12 (hIL-7/mIL-12-VV) is mostly suppressed by the depletion of CD8$^+$ T cells, indicating that subsets of CD8$^+$ T cells drive treatment efficacy. Here, we investigated the phenotypic changes in intratumoral CD8$^+$ T cells caused by treatment with hIL-7/mIL-12-VV or its backbone virus without IL-7 and IL-12 (Cont-VV) and found that these recombinant viruses increased expression of inducible co-stimulator (ICOS) in PD-1$^-$CD8$^+$ T cells. ICOS is a major marker of CD4$^+$ follicular helper T (T_{FH}) cells, which are crucial for the humoral immune response in secondary lymphoid organs.[17] A subset of CD8$^+$ T cells in chronic viral infection reportedly expresses ICOS together with CXCR5, also a known marker of T_{FH} cells, and shows minimal granzyme B expression.[18] CXCR5^{+-} ICOS$^+$CD8$^+$ T cells, which have been reported in patients with Hodgkin's lymphoma, show lower expression of IFN-γ, perforin, and

Received 21 December 2020; accepted 26 January 2021;
https://doi.org/10.1016/j.omto.2021.01.016.

Correspondence: Shinsuke Nakao, Drug Discovery Research, Astellas Pharma, Inc., 21, Miyukigaoka, Tsukuba 305-8585, Japan.
E-mail: shinsuke.nakao@astellas.com

granzyme B than CXCR5$^-$ICOS$^-$CD8$^+$ cells.[19] Treatment with an anti-CTLA4 antibody or oncolytic vaccinia virus reportedly upregulates ICOS expression in intratumoral CD8$^+$ T cells, while the impact on their effector phenotype remains unclear.[20–22] We found that, in contrast with these previous reports, a subset of intratumoral ICOS^{+-}PD-1$^-$CD8$^+$ T cells induced by hIL-7/mIL-12-VV or Cont-VV demonstrated an effector phenotype characterized by granzyme B expression. Our findings improve understanding of the heterogeneity of CD8$^+$ T cells and further support evaluation of this virotherapy in humans.

RESULTS

An oncolytic vaccinia virus carrying IL-7 and IL-12 enhanced intratumoral immune response and induced complete tumor regression (CR) in an immunocompetent mouse model

In this study, we used a recombinant oncolytic vaccinia virus that did not carry any immune transgene (Cont-VV), one carrying hIL-7 (hIL-7-VV), one carrying mIL-12 (mIL-12-VV), and one carrying both hIL-7 and mIL-12 (hIL-7/mIL-12-VV) (Figure 1A).[13] These viruses were based on LC16mO attenuated smallpox vaccine strain, with functional deletion of vaccinia virus growth factor (VGF) and O1L for tumor-selective viral replication.[23,24] In addition, B5R envelope glycoprotein was partially deleted to reduce antigenicity.[25,26] Cont-VV contained the gene for *Discosoma* sp. red fluorescent protein (DsRed) and luciferase in the VGF and O1L loci of the virus genome, respectively. Likewise, hIL-7-VV contained hIL-7 and lacZ, mIL-12-VV contained mIL-12 and luciferase genes, and hIL-7/mIL-12-VV contained hIL-7 and mIL-12 genes in the VGF and O1L loci, respectively. The culture supernatant of A549 cells infected with hIL-7-VV or hIL-7/mIL-12-VV, unlike that of cells infected with Cont-VV or mIL-12-VV, enhanced proliferation of mouse splenocytes (Figure S1A) because of the presence of hIL-7 protein in the supernatant, which is known to cross-react with mouse immune cells.[27] In contrast, the culture supernatant of A549 cells infected with mIL-12-VV or hIL-7/mIL-12-VV, unlike that of cells infected with Cont-VV or hIL-7-VV, induced release of murine IFN-γ from splenocytes (Figure S1B) as a result of the presence of mIL-12 protein in the supernatant. Consistent with our previous findings in the Lewis lung carcinoma (LLC) model lung carcinoma model,[13] intratumoral administration of hIL-7/mIL-12-VV in the CT26.WT colon carcinoma model caused release of hIL-7 and mIL-12 proteins in injected tumors (Figures 1B and 1C), with increased induction of intratumoral murine IFN-γ protein compared with Cont-VV (Figure 1D). Tumor-infiltrating CD4$^+$ T cells and CD8$^+$ T cells were also increased in mice treated with hIL-7/mIL-12-VV compared with mice treated with Cont-VV (Figures 1E and 1F), indicating that intratumoral IL-7 and IL-12 proteins promoted inflammatory responses in the tumor microenvironment. Increasing the dose of hIL-7/mIL-12-VV improved antitumor efficacy, and four out of six mice treated with 2×10^7 plaque-forming units (PFUs) of hIL-7/hIL-12-VV achieved CR (Figure 1G). Meanwhile, only partial tumor growth inhibition was observed in four out of six mice treated with Cont-VV at 2×10^7 PFUs, although the remaining two mice achieved CR (Figure 1H).

An oncolytic vaccinia virus increased ICOS$^+$PD-1$^-$CD8$^+$ effector T cells

We further investigated immune status changes in CT26.WT tumors after viral treatment. Because depletion of CD8$^+$ T cells, but not CD4$^+$ T cells, suppressed the antitumor efficacy of hIL-7/mIL-12-VV (Figure S2), we assumed that CD8$^+$ T cells may be key players in antitumor efficacy. Although an increased number of IL-7- and IL-12-induced tumor-infiltrating CD8$^+$ T cells may account for the superior efficacy of hIL-7/mIL-12-VV compared with Cont-VV, we examined the surface expression of various markers on intratumoral CD8$^+$ T cells to identify the phenotypic changes in CD8$^+$ T cells caused by hIL-7/mIL-12-VV or Cont-VV. First, we found that the proportion of PD-1-negative CD8$^+$ T cells increased after treatment with either hIL-7/mIL-12-VV or Cont-VV (Figures 2A and 2B). At the same time, hIL-7/mIL-12-VV, but not Cont-VV, upregulated PD-L1 on CT26.WT cells (Figure S3). Notably, most PD-1$^-$CD8$^+$ T cells showed ICOS expression 6 days after treatment with hIL-7/mIL-12-VV or Cont-VV, compared with less than half of PD-1$^-$CD8$^+$ T cells in mice that did not receive viral treatment (Figures 2A and 2C). Expression of T cell immunoglobulin (Ig) and mucin domain 3 (Tim-3) was also upregulated on PD-1$^-$CD8$^+$ T cells 6 days after viral treatment, although the percentage of Tim-3$^+$ T cells was lower than that of ICOS$^+$ T cells (Figure 2D; Figure S4). The ratio of PD-1$^-$CD8$^+$ T cells expressing the glucocorticoid-induced tumor necrosis factor (TNF) receptor family-regulated gene (GITR) and T cell immunoreceptor with Ig and immunoreceptor tyrosine–based inhibitory motif (ITIM) domains (TIGIT) was identical between virus-treated groups and the non-virus-treated group (Figures 2E and 2F; Figure S4). Almost all PD-1$^+$CD8$^+$ T cells showed ICOS expression regardless of the type of treatment, although lower percentages of ICOS$^+$ cells were observed in the vehicle group (Figure 2G). ICOS expression in PD-1$^-$CD8$^+$ T cells also was observed at the later time point (15 days after treatment), although the proportion of ICOS$^+$ cells was lower than that at the earlier time point (Figures 2H and 2I). We also observed increased ICOS expression in PD-1$^-$CD8$^+$ T cells after treatment with hIL-7/mIL-12-VV or Cont-VV in an LLC lung carcinoma mouse model (Figures 2J and 2K), suggesting that this phenotypic change may be caused by a common mechanism shared by these different mouse models. Taken together, our findings suggest that hIL-7/mIL-12-VV and Cont-VV induce similar phenotypic changes on intratumoral CD8$^+$ T cells, characterized by an increase in ICOS$^+$PD-1$^-$CD8$^+$ T cells.

Next, we examined the effector potential of ICOS$^-$ and ICOS$^+$ CD8$^+$ T cells. Six days after treatment with Cont-VV, the majority of ICOS^{+-}PD-1$^-$CD8$^+$ T cells, as well as ICOS$^+$PD-1$^+$CD8$^+$ T cells, showed granzyme B expression, compared with less than half of ICOS$^-$PD-1$^-$CD8$^+$ T cells (Figures 3A and 3B). Gp70-tetramer$^+$ tumor antigen-specific CD8$^+$ T cells showed a similar trend of higher granzyme B expression in ICOS$^+$CD8$^+$ T cells than ICOS$^-$CD8$^+$ T cells (Figure 3C). Granzyme B expression in ICOS$^+$CD8$^+$ T cells also was observed at the later time point (15 days after treatment), although the percentage of granzyme B-positive cells had decreased (Figures 3D–3F). Most ICOS$^+$CD8$^+$ T cells infiltrating LLC tumors also expressed granzyme B 6 days after treatment with Cont-VV (Figures

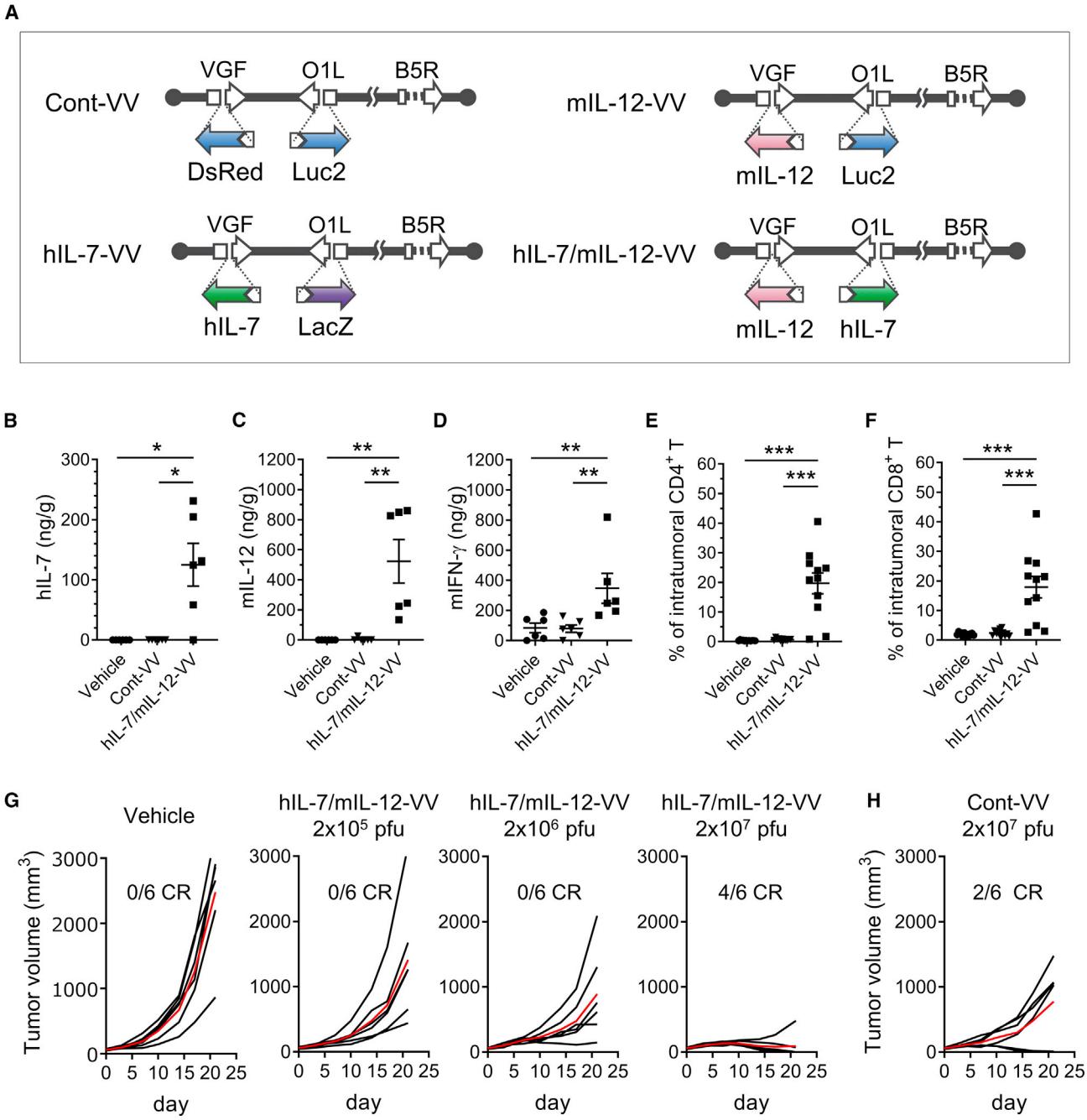

Figure 1. IL-7 and IL-12 encoded in an oncolytic vaccinia virus improves the immune status of tumors and induces complete tumor regression (CR)

(A) Schematic overview of Cont-VV, hIL-7-VV, mIL-12-VV, and hIL-7/mIL-12-VV. VGF and O1L are functionally deleted by insertion of transgenes as indicated. B5R is modified such that the short consensus repeat domains of B5R are deleted. (B–D) CT26.WT tumors on the right flank of BALB/c mice were treated with vehicle solution, 2×10^7 PFUs of Cont-VV, or 2×10^7 PFUs of hIL-7/mIL-12-VV (n = 6 per group). The day after treatment the tumors were collected, and the concentrations of hIL-7 (B), murine IL-12 (C), and murine IFN-γ (D) were measured. (E and F) Nineteen days after treatment, tumor-infiltrating $CD4^+$ T cells (E) and $CD8^+$ T cells (F) were analyzed by flow cytometry (n = 11–12). Data in (B)–(F) are mean ± SEM. *$p < 0.05$; **$p < 0.01$; ***$p < 0.001$ by Mann-Whitney U test. (G) Vehicle solution, hIL-7/mIL-12-VV at a dose of 2×10^5, 2×10^6, and 2×10^7 PFUs were intratumorally injected into CT26.WT tumors every other day, a total of three times. Growth of individual tumors in mice treated with vehicle or hIL-7/mIL-12-VV is shown. Mean tumor volume for each group is shown by the red line. Ratios of mice that achieved CR by day 28 are shown (n = 6). (H) 2×10^7 PFUs of Cont-VV was intratumorally injected as in (G). Growth of individual tumors in mice treated with Cont-VV is shown (n = 6).

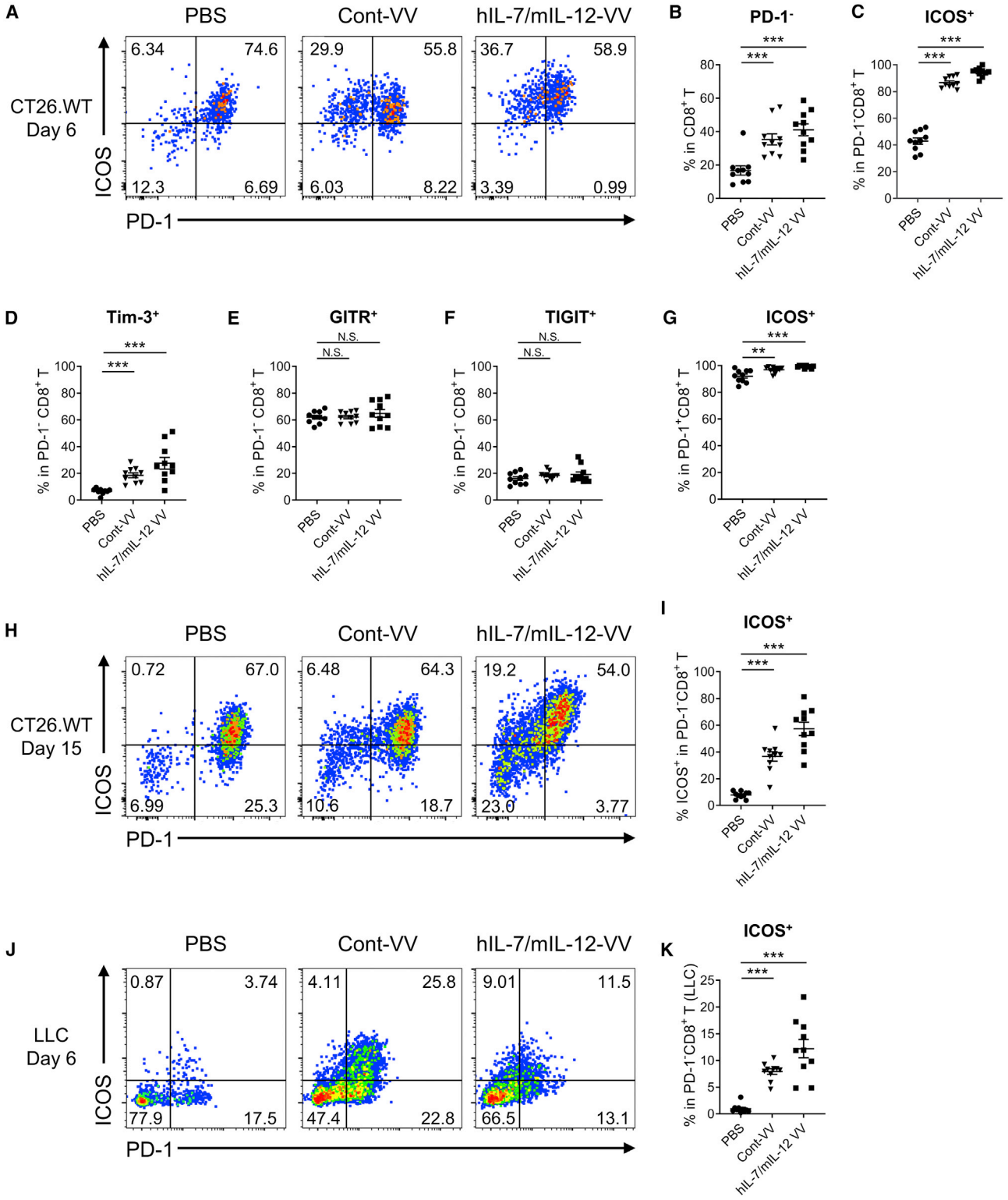

Figure 2. Intratumoral injection of Cont-VV or hIL-7/mIL-12-VV increases ICOS expression in PD-1⁻CD8⁺ T cells

(A–G) BALB/c mice bearing subcutaneous CT26.WT tumors (about 50 mm^3) were intratumorally injected with PBS, 2×10^7 PFUs of Cont-VV, or 2×10^7 PFUs of hIL-7/mIL-12-VV. Six days after treatment, tumor-infiltrating $CD8^+$ T cells were analyzed by flow cytometry (n = 10). (A) Representative plots of PD-1 and ICOS expression in intratumoral

(legend continued on next page)

3G and 3H). Likewise, a higher proportion of ICOS$^+$CD8$^+$ T cells than ICOS$^-$CD8$^+$ T cells in CT26.WT and LLC tumors treated with hIL-7/mIL-12-VV expressed granzyme B (Figure S5).

ICOS expression in PD-1$^-$CD8$^+$ effector T cells is independent of the type I IFN pathway

To identify the intratumoral immune pathways contributing to the induction of ICOS expression in PD-1$^-$CD8$^+$ T cells after virotherapy using this vaccinia virus platform, we conducted immune-related gene expression analysis of CT26.WT tumors treated with Cont-VV using a NanoString Pancancer Immune Profiling panel. Virus infection is known to activate the innate immune response, which is triggered by secretion of type I IFNs, IFN-α and IFN-β.[9] As expected, intratumoral treatment with Cont-VV markedly changed the expression levels of multiple immune-related genes and upregulated various immune pathways (Figures 4A and 4B), including type I IFN and innate pathways (Figure 4C). In fact, the top 20 most significantly upregulated genes in Cont-VV-injected CT26.WT tumors were mostly IFN-inducible genes, downstream molecules of the type I IFN receptor (Table 1), suggesting that Cont-VV directly or indirectly induced type I IFNs. These findings prompted us to examine whether upregulation of ICOS expression in PD-1$^-$CD8$^+$ T cells is mediated by type I IFN signaling. Although inhibition of type I IFN signaling with anti-IFN-α/β receptor (IFNR) antibody partially blocked antitumor immunity characterized by a decrease in the number of tumor-infiltrating CD8$^+$ T cells (Figure 5A) and enhanced tumor growth (Figure 5B), ICOS expression in PD-1$^-$CD8$^+$ T cells did not decrease after treatment with Cont-VV (Figures 5C and 5D), suggesting that ICOS upregulation in PD-1$^-$CD8$^+$ T cells is independent of the type I IFN pathway.

DISCUSSION

Immune checkpoint inhibitors have provided marked clinical benefits and improved overall survival for patients with solid tumors. However, clinical efficacy remains limited to a subset of patients. To further improve the clinical response rate, a large number of clinical trials are now actively testing a combination of immune checkpoint blockade with other approaches, including chemotherapy, radiotherapy, targeted therapy, and other immunotherapies.[28] We previously proposed *in situ* vaccination using an oncolytic vaccinia virus carrying IL-7 and IL-12 as a promising antitumor approach and demonstrated its usefulness in combination with anti-PD-1 or anti-CTLA4 antibody.[13] Here, we conducted a detailed investigation of the phenotypic changes in intratumoral CD8$^+$ T cells after treatment with this virotherapy and identified a marked increase in a previously unidentified PD-1$^-$CD8$^+$ effector T cell subset characterized by ICOS expression. ICOS was predominantly thought to be an activation marker associated with CD4$^+$ follicular T cells in germinal centers[29,30]; however, recent studies have expanded our understanding of ICOS$^+$ T cells in peripheral blood and tumor tissues. Treatment with anti-CTLA4 antibody has been shown to increase the frequency of IFN-γ-producing ICOS$^+$CD4$^+$ T cells in peripheral blood and tumors in patients with bladder cancer.[31] Sustained levels of ICOS$^+$CD4$^+$ T cells in peripheral blood after treatment with anti-CTLA4 antibody correlate with the expected clinical benefits.[32] ICOS$^+$CD8$^+$ T cells have also been reported in humans and mouse models, with ICOS$^+$PD-1$^-$CD8$^+$ T cells in syngeneic mouse models reported to show low granzyme B and IFN-γ expression.[33] In our study, we also observed ICOS expression in CD8$^+$ T cells. However, ICOS$^+$PD-1$^-$CD8$^+$ T cells induced by treatment with hIL-7/mIL-12-VV or Cont-VV were qualitatively different from those reported previously, showing an effector phenotype characterized by granzyme B expression. Regarding the ICOS$^+$PD-1$^-$ phenotype, we assume that this cell subset is similar to CD45RO$^+$ICOS$^+$PD-1^{low}CD4$^+$ T cells in human melanoma tissues, the number of which has been shown to increase following treatment with an anti-CTLA4 antibody.[34] Expression of granzyme B was also observed in ICOS$^+$PD-1$^+$CD8$^+$ T cells, but not ICOS$^-$CD8$^+$ T cells, suggesting that ICOS$^+$ T cells may be the drivers of the antitumor efficacy of hIL-7/mIL-12-VV and Cont-VV. It is likely that the greater number of tumor-infiltrating ICOS$^+$CD8$^+$ T cells after treatment with hIL-7/mIL-12-VV compared with Cont-VV may contribute to the stronger antitumor efficacy of hIL-7/mIL-12-VV. In addition, we assume that the increase in ICOS$^+$PD-1$^-$CD8$^+$ effector T cells is important because this subset may evade inactivation by the PD-1/PD-L1 axis.

It is of note that ICOS expression in PD-1$^-$CD8$^+$T cells was induced by not only hIL-7/mIL-12-VV but also Cont-VV, an oncolytic vaccinia virus with no immunomodulatory molecule. Vaccinia viruses are known to have the potential to activate innate immune responses, including those linked to the type I IFN pathway.[9] In particular, replication-competent oncolytic vaccinia viruses can induce immunogenic cell death of cancer cells, which triggers the type I IFN pathway through the cyclic GMP-AMP synthase/stimulator of IFN gene (cGAS/STING) axis.[35,36] As expected, intratumoral treatment with Cont-VV upregulated multiple genes in the type I IFN pathway in tumors. Considering that the virus backbone LC16mO and its parent strain Lister are deficient in B18R vaccinia virus protein, which works as a decoy receptor for type I IFNs,[37,38] it is plausible that loss of B18R positively contributes to upregulation of the type I IFN pathway. However, unexpectedly, we found that ICOS

CD8$^+$ T cells. (B) Percentage of PD-1$^-$ cells in intratumoral CD8$^+$ T cells. (C) Percentage of ICOS$^+$ cells in intratumoral PD-1$^-$CD8$^+$ T cells. (D–F) Percentage of Tim-3$^+$ cells (D), GITR$^+$ cells (E), and TIGIT$^+$ cells (F) in intratumoral PD-1$^-$CD8$^+$ T cells. (G) Percentage of ICOS$^+$ cells in intratumoral PD-1$^+$CD8$^+$ T cells. (H and I) CT26.WT tumors were treated with PBS, 2×10^7 PFUs of Cont-VV, or 2×10^7 PFUs of hIL-7/mIL-12-VV every other day for a total of three times. Tumors were collected 15 days after the first treatment, and intratumoral CD8$^+$ T cells were analyzed by flow cytometry (n = 10). (H) Representative plots of PD-1 and ICOS expression. (I) Percentage of ICOS$^+$ cells in PD-1$^-$CD8$^+$ T cells. (J and K) LLC tumors in C57BL/6 mice were treated with PBS, 2×10^7 PFUs of Cont-VV, or 2×10^7 PFUs of hIL-7/mIL-12-VV. Tumors were collected 6 days after treatment, and intratumoral CD8$^+$ T cells were analyzed (n = 10). (J) Representative plots of PD-1 and ICOS expression. (K) Percentage of ICOS$^+$ cells in PD-1$^-$CD8$^+$ T cells. Mean ± SEM is shown. $^{**}p < 0.01$; $^{***}p < 0.001$ by Mann-Whitney U test. N.S., not significant.

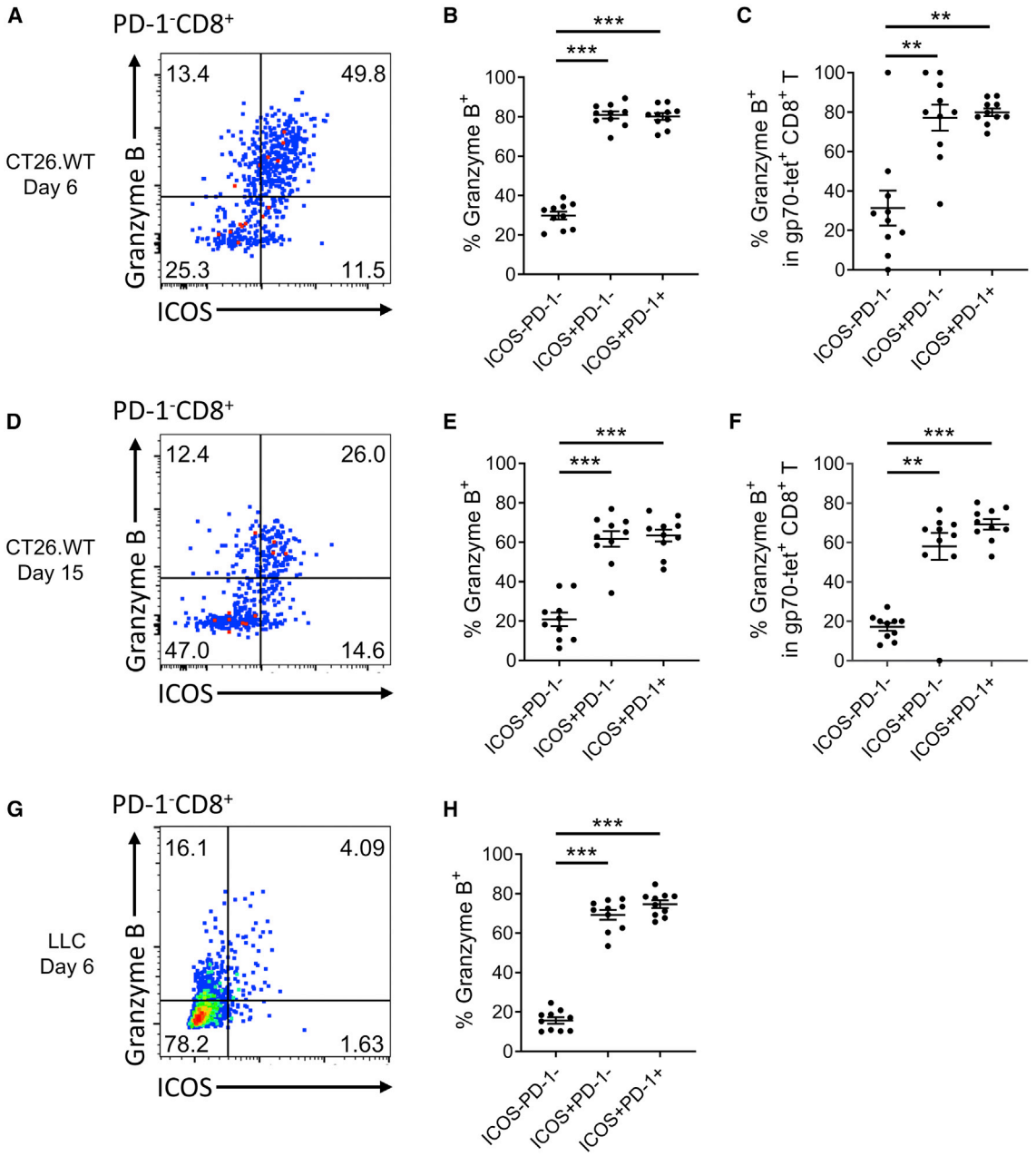

Figure 3. ICOS$^+$PD-1$^-$CD8$^+$ T cells induced by Cont-VV show granzyme B expression

(A–F) BALB/c mice bearing subcutaneous CT26.WT tumors were intratumorally injected with Cont-VV as described in Figure 2. Tumors were collected 6 (A–C) or 15 (D–F) days after treatment (n = 10 per group). (A and D) Representative plots of granzyme B and ICOS expression in intratumoral PD-1$^-$CD8$^+$ T cells. (B and E) Expression of granzyme B in intratumoral ICOS$^-$PD-1$^-$CD8$^+$ T cells, ICOS$^+$PD-1$^-$CD8$^+$ T cells, and ICOS$^+$PD-1$^+$CD8$^+$ T cells. (C and F) Expression of granzyme B in gp70-tetramer$^+$ tumor antigen-specific CD8$^+$ T cells. (G and H) LLC tumors treated with Cont-VV were collected 6 days after treatment, and tumor-infiltrating CD8$^+$ T cells were analyzed (n = 10). (G) Representative plots of granzyme B and ICOS expression in intratumoral PD-1$^-$CD8$^+$ T cells. (H) Expression of granzyme B in each indicated subset. Mean ± SEM is shown. **p < 0.01; ***p < 0.001 by Mann-Whitney U test.

expression in PD-1$^-$CD8$^+$ T cells induced by Cont-VV was independent of the type I IFN pathway, suggesting that yet-to-be identified soluble factors or cell-to-cell stimuli may work on intratumoral PD-1$^-$CD8$^+$ T cells.

We acknowledge there are some limitations of this study that prevented us from obtaining a full understanding of ICOS induction by hIL-7/mIL-12-VV and Cont-VV. First, although we demonstrated that the type I IFN pathway is not essential, further studies are needed to

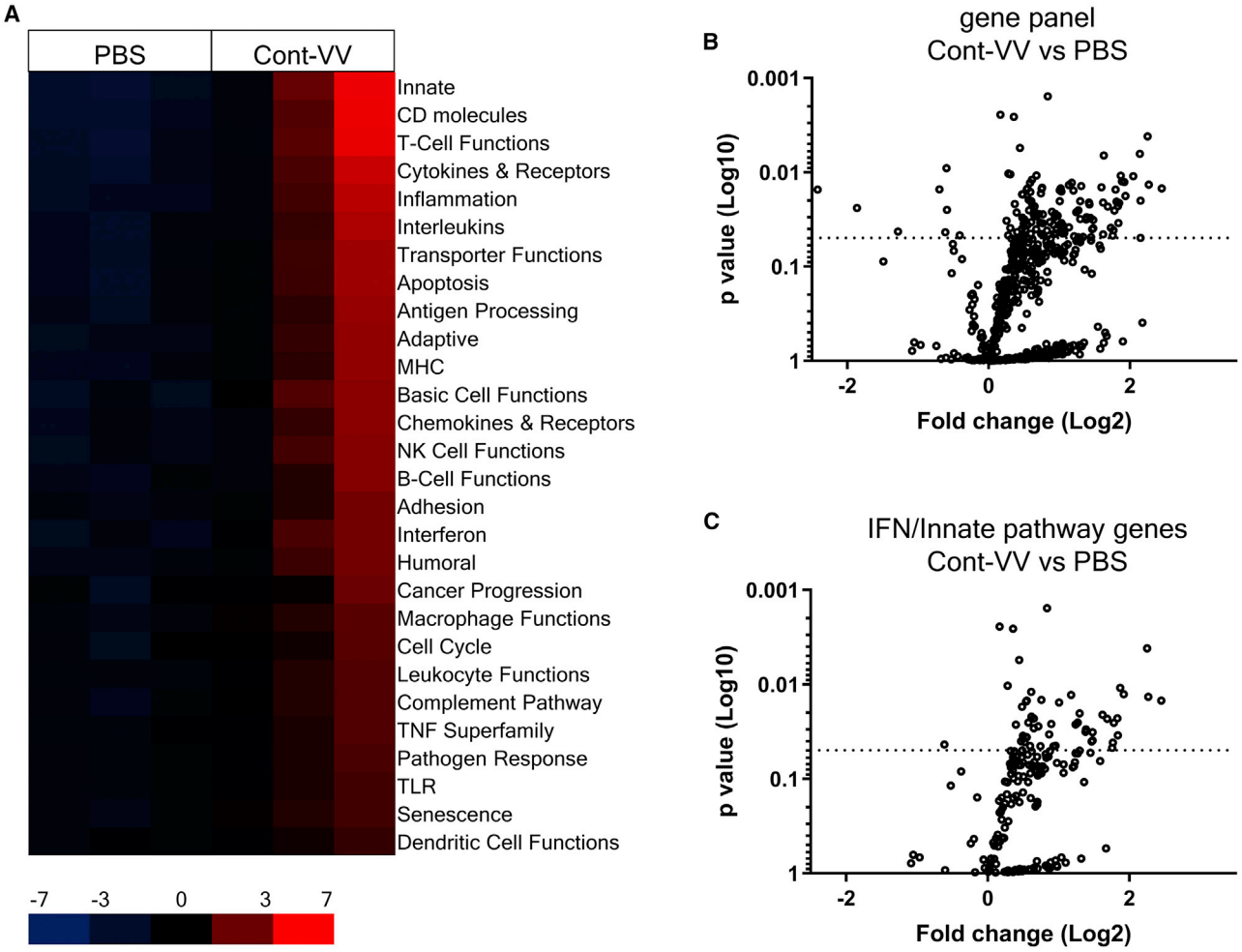

Figure 4. Intratumoral injection of Cont-VV upregulates multiple immune pathways

BALB/c mice bearing CT26.WT tumors were intratumorally injected with PBS or 2×10^7 PFUs of Cont-VV. Two days after treatment, tumors were collected, and RNA was isolated and analyzed using the PanCancer Mouse Immune Profiling panel. (A) Expression profile of immune-related pathways. Red indicates high expression, and blue indicates low expression. (B) Volcano plots of all genes assessed that are upregulated or downregulated by Cont-VV. (C) Volcano plots of genes related to IFN and innate pathways.

elucidate the molecular mechanisms contributing to the increase in $ICOS^+PD\text{-}1^-CD8^+$ T cells after viral treatment. TLR signaling that can be stimulated by DAMPs from killed cells[39] may be another candidate. Moreover, differential gene analysis of $ICOS^+PD\text{-}1^-CD8^+$ T cells compared with $ICOS^-PD\text{-}1^-CD8^+$ T cells will also provide valuable clues. Second, we did not evaluate whether ICOS induction and its underlying mechanism are common among vaccinia virus strains. This is an important future study considering that our vaccinia virus platform, which is based on LC16mO, induced minimum levels of IFN-γ (Figure 1D) and PD-L1 (Figure S3), while a previous study using a vaccinia virus based on Western Reserve strain showed a greater effect.[21] Finally, we did not precisely characterize the differentiation status of $ICOS^+CD8^+$ T cells. Future studies should do so by assessing the expression levels of effector and memory T cell markers, such as T-box in T cells (T-bet) and eomesodermin (Eomes),[40] and elucidate the antitumor effects of ICOS in virotherapy, given that increased expression of ICOS in $CD8^+$ T cells has been reported to play a crucial role in the antitumor efficacy of anti-CTLA4 antibody.[20,22]

Taken together, our data demonstrate that intratumoral treatment with an oncolytic vaccinia virus increases a previously unidentified $ICOS^+PD\text{-}1^-CD8^+$ effector T cell subset. Understanding the phenotypic changes in $CD8^+$ T cells caused by an oncolytic vaccinia virus carrying IL-7 and IL-12 may provide a scientific rationale to support further evaluation in humans.

MATERIALS AND METHODS

Virus construction

As described previously, a plasmid containing DsRed gene connected to the p7.5 promoter and a plasmid containing luciferase gene connected to a synthetic vaccinia virus promoter (SP)[41] were used to construct Cont-VV.[13] Likewise, a plasmid containing hIL-7 gene

Table 1. Top 20 genes upregulated in CT26.WT tumors treated with Cont-VV

Probe	Log2-fold change	Lower confidence limit (log2)	Upper confidence limit (log2)	p value
Mx2[a]	2.45	1.28	3.62	0.0148
Ifit3[a]	2.27	1.22	3.33	0.0135
Irf7[a]	2.25	1.5	3	0.00415
Tap2	2.15	0.637	3.66	0.0496
Gzma	2.15	1.03	3.27	0.02
Usp18[a]	2.14	1.34	2.94	0.00635
Oasl1[a]	2.05	1.15	2.94	0.011
H2-T23	1.94	0.959	2.91	0.0178
Isg15[a]	1.92	1.04	2.8	0.0127
Xaf1[a]	1.89	1.03	2.75	0.0125
Bst2[a]	1.87	1.05	2.68	0.0109
Siglec1[a]	1.85	0.867	2.84	0.0212
Cxcl10[a]	1.84	0.694	2.98	0.0345
Zbp1[a]	1.83	0.835	2.83	0.0228
Il2rb	1.81	0.854	2.76	0.0205
Rsad2[a]	1.8	0.931	2.67	0.0153
Ifi44l[a]	1.78	0.778	2.79	0.0255
Cxcl11[a]	1.77	0.6	2.93	0.0413
Nod1	1.76	0.543	2.97	0.047
Psmb9	1.73	0.609	2.85	0.0389

[a]IFN-inducible genes, downstream molecules of the type I IFN receptor.

connected to SP and a plasmid containing LacZ connected to SP were used for hIL-7-VV; a plasmid containing mIL-12 gene connected to SP and a plasmid containing luciferase connected to SP were used for mIL-12-VV; a plasmid containing mIL-12 gene connected to SP and a plasmid containing hIL-7 gene connected to SP were used for hIL-7/mIL-12-VV. For virus recombination, RK13 cells were infected with the LC16mO strain modified by functional deletion of VGF and O1L and partial deletion of B5R glycoprotein,[13] then transfected with each plasmid. Infected cells were harvested, and recombined viruses were selected and purified as described previously.[26] All viruses were propagated in RK13 or A549 cells and concentrated by density gradient ultracentrifugation using OptiPrep (Axis-Shield, Dundee, Scotland) or tangential flow filtration, then titrated using a standard plaque assay as described previously.[13] They were stored at −80°C until just before use.

Cell lines

Rabbit kidney RK13 (CCL-37), human lung carcinoma A549 (CCL-185), murine colon carcinoma CT26.WT (CRL-2638), and murine lung carcinoma LLC (CRL-1642) were purchased from American Type Culture Collection (ATCC, Manassas, VA, USA). RK13 was cultured in Eagle's minimum essential medium (ATCC) supplemented with 10% heat-inactivated fetal bovine serum and penicillin-streptomycin (Thermo Fisher Scientific, Waltham, MA, USA). A549 was cultured in F-12K medium (ATCC) or Dulbecco's modified Eagle's medium (DMEM; Merck, Darmstadt, Germany) supplemented with 10% heat-inactivated fetal bovine serum and penicillin-streptomycin. CT26.WT was cultured in RPMI-1640 medium (Merck) supplemented with 10% heat-inactivated fetal bovine serum, 10 mmol/L HEPES, 1 mmol/L sodium pyruvate, and 4,500 mg/L glucose and penicillin-streptomycin. LLC was cultured in DMEM supplemented with 10% heat-inactivated fetal bovine serum and penicillin-streptomycin. All cell lines were tested and confirmed to be mycoplasma free. All cells were cultured at 37°C in a 5% CO_2 humidified atmosphere.

Animal experiments

All animal procedures and experiments were approved by the Institutional Animal Care and Use Committee of Astellas Pharma, Tsukuba Research Center, which is accredited by AAALAC International. BALB/c mice and C57BL/6 mice were purchased from Charles River Laboratories Japan. They were maintained on a standard diet and water *ad libitum* throughout the experiments under specific pathogen-free conditions. For evaluation of antitumor activity and immune response, mice bearing CT26.WT or LLC were used. In brief, 3×10^5 to 6×10^5 cells were subcutaneously inoculated into the right flank of mice. Tumor diameter was measured using a digital caliper, and tumor volume was calculated using the formula length × width^2 × 0.52. When tumors reached about 50 mm^3, mice were randomly allocated to experimental groups such that mean tumor volumes were similar in each group, and 30 μL of vehicle solution or virus suspension was injected intratumorally. When tumors could no longer be detected by palpation, mice were defined as having achieved CR. Schedules, the number of animals per group, and statistical tests used for each experiment are described in the figure legends. For deletion of $CD8^+$ and $CD4^+$ T cells, 200 μg/mouse of anti-CD8 antibody (clone 53-6.72; ATCC) and anti-CD4 antibody (clone GK1.5; Bio X Cell, West Lebanon, NH, USA) were used, respectively. These antibodies were intraperitoneally administered on days 1 (first day of viral treatment), 2, 3, 6, and 9. For blockade of the type I IFN pathway, anti-IFNR antibody (clone MAR1-5A3; Bio X Cell) was used, and mouse IgG1 (clone MOPC-21 Bio X Cell) was used as a negative control. These antibodies were intraperitoneally administered at 500 μg/mouse 1 day before the viral treatment (day 0) and on days 1 and 2, and then at 250 μg/mouse on days 3, 5, and 7.

Flow cytometry

Tumor tissues were collected and suspended using the Mouse Tumor Dissociation Kit (Miltenyi Biotec, Bergisch Gladbach, Germany). Cells were stained with the following antibodies: mouse TIGIT BV421, mouse GITR V510, mouse ICOS BB515, mouse PD-1 allophycocyanin (APC), mouse CD8a V500 (BD Biosciences, San Jose, CA, USA); mouse CD45 Alexa Fluor 647, mouse CD4 fluorescein isothiocyanate (FITC), mouse CD8a PerCP-Cy5.5, mouse PD-1 PE-Cy7, mouse granzyme B Alexa Fluor 647, mouse granzyme B FITC, mouse CD274 BV421, mouse ICOS PerCP-Cy5.5 (BioLegend, San Diego, CA, USA); mouse Tim-3 PE (Thermo Fisher Scientific); and PE-labeled gp70 tetramer (Medical & Biological Laboratories, Aichi,

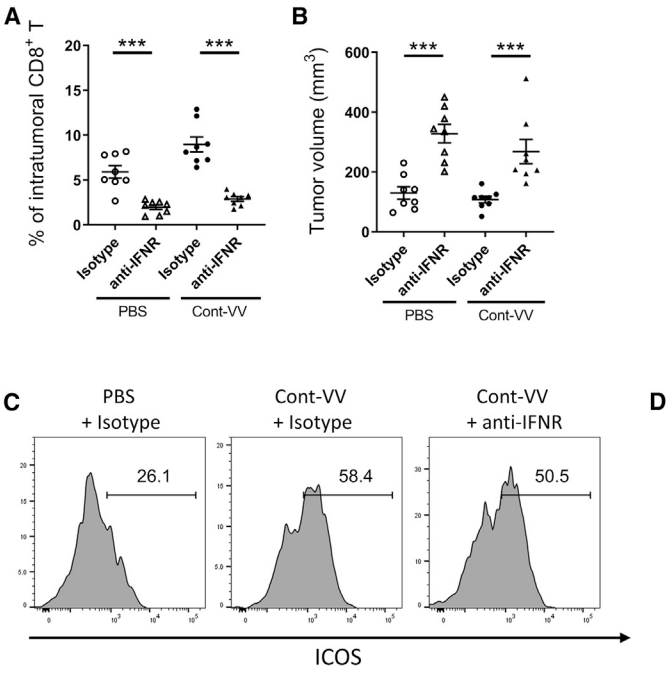

Figure 5. ICOS expression in PD-1^{-}CD8^{+} T cells is independent of type I IFN signaling

BALB/c mice bearing subcutaneous CT26.WT tumors were intratumorally injected with PBS or Cont-VV, with or without blockade of type I IFNs. Seven days after viral treatment (n = 8 per group), intratumoral CD8^{+} T cells were analyzed using flow cytometry. (A) Percentage of intratumoral CD8^{+} T cells. (B) Tumor volume on the day of tumor collection. (C) Representative fluorescence intensity of ICOS expression in PD-1^{-}CD8^{+} T cells. (D) Percentage of ICOS^{+} cells in intratumoral PD-1^{-}CD8^{+} T cells. Mean ± SEM is shown. ***p < 0.001 by Mann-Whitney U test. N.S., not significant.

Japan). BD fixation/permeabilization kit (BD Biosciences) was used for intracellular staining. Fixable Viability Dye eFluor 780 (Thermo Fisher Scientific) or Zombie NIR (BioLegend) was used to identify dead cells. All samples were analyzed by flow cytometry using a MACSQuant Analyzer 10 (Miltenyi Biotec). Acquired data were analyzed using FlowJo v.10 (BD Biosciences).

Measurement of intratumoral cytokines

Tumor tissues were collected the day after viral treatment and immediately frozen. Samples were suspended in T-PER Buffer (Thermo Fisher Scientific) using the gentleMACS Dissociator (Miltenyi Biotec). Concentrations of hIL-7, mIL-12, and murine IFN-γ in tumor lysate were measured using the RayBio Human IL-7 ELISA Kit (Ray Biotech, Norcross, GA, USA), Quantikine ELISA Mouse IL-12 p70 Immunoassay (R&D Systems, Minneapolis, MN, USA), and Quantikine ELISA Mouse IFN-γ Immunoassay (R&D Systems), respectively. Concentrations of cytokines were normalized to those of total protein, which was measured using Pierce 660-nm Protein Assay Reagent (Thermo Fisher Scientific). Measurement was conducted on the EnSpire multimode plate reader (Perkin Elmer, Waltham, MA, USA).

Ex vivo analysis of immune response

A549 was infected with Cont-VV, hIL-7-VV, mIL-12-VV, or hIL-7/mIL-12-VV at a multiplicity of infection (MOI) of 1.0. Two days later, the supernatants were collected and filtered through a 0.1-μm polyvinylidene fluoride (PVDF) membrane (Millipore, Burlington MA, USA). Serially diluted supernatants were added to 1×10^5 C57BL/6 mouse splenocytes in a 96-well plate. Three days later, secretion of murine IFN-γ was assessed using Quantikine ELISA Mouse IFN-γ Immunoassay (R&D Systems), and the proliferation of splenocytes was assessed using CellTiter-Glo (Promega, Fitchburg, WI, USA). Measurement was conducted on an EnSpire multimode plate reader.

Gene expression analysis

BALB/c mice bearing CT26.WT tumors were intratumorally treated with PBS or 2×10^7 PFUs of Cont-VV. Tumors were collected 2 days after treatment. RNA extracted from tumors was examined using the PanCancer Mouse Immune Profiling Panel (NanoString Technologies, Seattle, WA, USA) and measured using the Digital Analyzer (nCounter). Data were processed using nSolver Analysis Software and the Advanced Analysis module (NanoString Technologies).

Statistical analysis

Statistical analysis was conducted using GraphPad Prism 8 (GraphPad Software, San Diego, CA, USA). Procedures for comparison and the number of animals in each experiment are described in each figure legend. The p values <0.05 were considered significant.

SUPPLEMENTAL INFORMATION

Supplemental Information can be found online at https://doi.org/10.1016/j.omto.2021.01.016.

ACKNOWLEDGMENTS

We thank M. Urio for technical assistance with the experiments. We thank M. Mori and T. Yoshida for scientific discussion. This research is funded by Astellas Pharma, Inc., Japan.

AUTHOR CONTRIBUTIONS

Conception and design: M.Y. and S.N.; development of methodology: M.Y., M.T., R.M., Y.A., T.N., and S.N.; acquisition of data: M.Y., M.T., R.M., Y.A., and S.N.; analysis and interpretation of data: M.Y., T.N., and S.N.; writing, review, and/or revision of the manuscript: M.Y. and S.N.; administrative, technical, or material support: T.N.; study supervision: S.N.

DECLARATION OF INTERESTS

M.Y., M.T., R.M., Y.A., and S.N. are employees of Astellas Pharma Inc., Japan. S.N. and T.N. are inventors named on the patent for recombinant oncolytic vaccinia viruses submitted by Astellas Pharma and Tottori University (US patent publication no. US 2017/0340687, published November 20, 2017).

REFERENCES

1. Hodi, F.S., O'Day, S.J., McDermott, D.F., Weber, R.W., Sosman, J.A., Haanen, J.B., Gonzalez, R., Robert, C., Schadendorf, D., Hassel, J.C., et al. (2010). Improved survival with ipilimumab in patients with metastatic melanoma. N. Engl. J. Med. *363*, 711–723.
2. Topalian, S.L., Hodi, F.S., Brahmer, J.R., Gettinger, S.N., Smith, D.C., McDermott, D.F., Powderly, J.D., Carvajal, R.D., Sosman, J.A., Atkins, M.B., et al. (2012). Safety, activity, and immune correlates of anti-PD-1 antibody in cancer. N. Engl. J. Med. *366*, 2443–2454.
3. Garon, E.B., Rizvi, N.A., Hui, R., Leighl, N., Balmanoukian, A.S., Eder, J.P., Patnaik, A., Aggarwal, C., Gubens, M., Horn, L., et al.; KEYNOTE-001 Investigators (2015). Pembrolizumab for the treatment of non-small-cell lung cancer. N. Engl. J. Med. *372*, 2018–2028.
4. Larkin, J., Chiarion-Sileni, V., Gonzalez, R., Grob, J.J., Rutkowski, P., Lao, C.D., Cowey, C.L., Schadendorf, D., Wagstaff, J., Dummer, R., et al. (2019). Five-Year Survival with Combined Nivolumab and Ipilimumab in Advanced Melanoma. N. Engl. J. Med. *381*, 1535–1546.
5. Ribas, A., and Wolchok, J.D. (2018). Cancer immunotherapy using checkpoint blockade. Science *359*, 1350–1355.
6. Galluzzi, L., Chan, T.A., Kroemer, G., Wolchok, J.D., and López-Soto, A. (2018). The hallmarks of successful anticancer immunotherapy. Sci. Transl. Med. *10*, eaat7807.
7. Chen, D.S., and Mellman, I. (2017). Elements of cancer immunity and the cancer-immune set point. Nature *541*, 321–330.
8. Schmidt, C. (2017). The benefits of immunotherapy combinations. Nature *552*, S67–S69.
9. Russell, S.J., and Barber, G.N. (2018). Oncolytic Viruses as Antigen-Agnostic Cancer Vaccines. Cancer Cell *33*, 599–605.
10. Liu, B.L., Robinson, M., Han, Z.Q., Branston, R.H., English, C., Reay, P., McGrath, Y., Thomas, S.K., Thornton, M., Bullock, P., et al. (2003). ICP34.5 deleted herpes simplex virus with enhanced oncolytic, immune stimulating, and anti-tumour properties. Gene Ther. *10*, 292–303.
11. Andtbacka, R.H., Ross, M., Puzanov, I., Milhem, M., Collichio, F., Delman, K.A., Amatruda, T., Zager, J.S., Cranmer, L., Hsueh, E., et al. (2016). Patterns of Clinical Response with Talimogene Laherparepvec (T-VEC) in Patients with Melanoma Treated in the OPTiM Phase III Clinical Trial. Ann. Surg. Oncol. *23*, 4169–4177.
12. Harrington, K., Freeman, D.J., Kelly, B., Harper, J., and Soria, J.C. (2019). Optimizing oncolytic virotherapy in cancer treatment. Nat. Rev. Drug Discov. *18*, 689–706.
13. Nakao, S., Arai, Y., Tasaki, M., Yamashita, M., Murakami, R., Kawase, T., Amino, N., Nakatake, M., Kurosaki, H., Mori, M., et al. (2020). Intratumoral expression of IL-7 and IL-12 using an oncolytic virus increases systemic sensitivity to immune checkpoint blockade. Sci. Transl. Med. *12*, eaax7992.
14. Gao, J., Zhao, L., Wan, Y.Y., and Zhu, B. (2015). Mechanism of Action of IL-7 and Its Potential Applications and Limitations in Cancer Immunotherapy. Int. J. Mol. Sci. *16*, 10267–10280.
15. Pellegrini, M., Calzascia, T., Elford, A.R., Shahinian, A., Lin, A.E., Dissanayake, D., Dhanji, S., Nguyen, L.T., Gronski, M.A., Morre, M., et al. (2009). Adjuvant IL-7 antagonizes multiple cellular and molecular inhibitory networks to enhance immunotherapies. Nat. Med. *15*, 528–536.
16. Lasek, W., Zagożdżon, R., and Jakobisiak, M. (2014). Interleukin 12: still a promising candidate for tumor immunotherapy? Cancer Immunol. Immunother. *63*, 419–435.
17. Hutloff, A., Dittrich, A.M., Beier, K.C., Eljaschewitsch, B., Kraft, R., Anagnostopoulos, I., and Kroczek, R.A. (1999). ICOS is an inducible T-cell co-stimulator structurally and functionally related to CD28. Nature *397*, 263–266.
18. Im, S.J., Hashimoto, M., Gerner, M.Y., Lee, J., Kissick, H.T., Burger, M.C., Shan, Q., Hale, J.S., Lee, J., Nasti, T.H., et al. (2016). Defining CD8+ T cells that provide the proliferative burst after PD-1 therapy. Nature *537*, 417–421.
19. Le, K.S., Amé-Thomas, P., Tarte, K., Gondois-Rey, F., Granjeaud, S., Orlanducci, F., Foucher, E.D., Broussais, F., Bouabdallah, R., Fest, T., et al. (2018). CXCR5 and ICOS expression identifies a CD8 T-cell subset with T_{FH} features in Hodgkin lymphomas. Blood Adv. *2*, 1889–1900.
20. Fan, X., Quezada, S.A., Sepulveda, M.A., Sharma, P., and Allison, J.P. (2014). Engagement of the ICOS pathway markedly enhances efficacy of CTLA-4 blockade in cancer immunotherapy. J. Exp. Med. *211*, 715–725.
21. Liu, Z., Ravindranathan, R., Kalinski, P., Guo, Z.S., and Bartlett, D.L. (2017). Rational combination of oncolytic vaccinia virus and PD-L1 blockade works synergistically to enhance therapeutic efficacy. Nat. Commun. *8*, 14754.
22. Shi, L.Z., Goswami, S., Fu, T., Guan, B., Chen, J., Xiong, L., Zhang, J., Ng Tang, D., Zhang, X., Vence, L., et al. (2019). Blockade of CTLA-4 and PD-1 Enhances Adoptive T-cell Therapy Efficacy in an ICOS-Mediated Manner. Cancer Immunol. Res. *7*, 1803–1812.
23. McCart, J.A., Ward, J.M., Lee, J., Hu, Y., Alexander, H.R., Libutti, S.K., Moss, B., and Bartlett, D.L. (2001). Systemic cancer therapy with a tumor-selective vaccinia virus mutant lacking thymidine kinase and vaccinia growth factor genes. Cancer Res. *61*, 8751–8757.
24. Schweneker, M., Lukassen, S., Späth, M., Wolferstätter, M., Babel, E., Brinkmann, K., Wielert, U., Chaplin, P., Suter, M., and Hausmann, J. (2012). The vaccinia virus O1 protein is required for sustained activation of extracellular signal-regulated kinase 1/2 and promotes viral virulence. J. Virol. *86*, 2323–2336.
25. Herrera, E., Lorenzo, M.M., Blasco, R., and Isaacs, S.N. (1998). Functional analysis of vaccinia virus B5R protein: essential role in virus envelopment is independent of a large portion of the extracellular domain. J. Virol. *72*, 294–302.
26. Nakatake, M., Kurosaki, H., Kuwano, N., Horita, K., Ito, M., Kono, H., Okamura, T., Hasegawa, K., Yasutomi, Y., and Nakamura, T. (2019). Partial Deletion of Glycoprotein B5R Enhances Vaccinia Virus Neutralization Escape while Preserving Oncolytic Function. Mol. Ther. Oncolytics *14*, 159–171.
27. Faltynek, C.R., Wang, S., Miller, D., Young, E., Tiberio, L., Kross, K., Kelley, M., and Kloszewski, E. (1992). Administration of human recombinant IL-7 to normal and irradiated mice increases the numbers of lymphocytes and some immature cells of the myeloid lineage. J. Immunol. *149*, 1276–1282.
28. Zappasodi, R., Merghoub, T., and Wolchok, J.D. (2018). Emerging Concepts for Immune Checkpoint Blockade-Based Combination Therapies. Cancer Cell *33*, 581–598.
29. Bauquet, A.T., Jin, H., Paterson, A.M., Mitsdoerffer, M., Ho, I.C., Sharpe, A.H., and Kuchroo, V.K. (2009). The costimulatory molecule ICOS regulates the expression of c-Maf and IL-21 in the development of follicular T helper cells and TH-17 cells. Nat. Immunol. *10*, 167–175.
30. Akiba, H., Takeda, K., Kojima, Y., Usui, Y., Harada, N., Yamazaki, T., Ma, J., Tezuka, K., Yagita, H., and Okumura, K. (2005). The role of ICOS in the CXCR5+ follicular B helper T cell maintenance in vivo. J. Immunol. *175*, 2340–2348.
31. Liakou, C.I., Kamat, A., Tang, D.N., Chen, H., Sun, J., Troncoso, P., Logothetis, C., and Sharma, P. (2008). CTLA-4 blockade increases IFNgamma-producing CD4+ICOShi cells to shift the ratio of effector to regulatory T cells in cancer patients. Proc. Natl. Acad. Sci. USA *105*, 14987–14992.
32. Carthon, B.C., Wolchok, J.D., Yuan, J., Kamat, A., Ng Tang, D.S., Sun, J., Ku, G., Troncoso, P., Logothetis, C.J., Allison, J.P., et al. (2010). Preoperative CTLA-4 blockade: tolerability and immune monitoring in the setting of a presurgical clinical trial. Clin. Cancer Res. *16*, 2861–2871.
33. Xiong, H., Mittman, S., Rodriguez, R., Pacheco-Sanchez, P., Moskalenko, M., Yang, Y., Elstrott, J., Ritter, A.T., Müller, S., Nickles, D., et al. (2019). Coexpression of Inhibitory Receptors Enriches for Activated and Functional $CD8^+$ T Cells in Murine Syngeneic Tumor Models. Cancer Immunol. Res. *7*, 963–976.
34. Wei, S.C., Levine, J.H., Cogdill, A.P., Zhao, Y., Anang, N.A.S., Andrews, M.C., Sharma, P., Wang, J., Wargo, J.A., Pe'er, D., and Allison, J.P. (2017). Distinct Cellular Mechanisms Underlie Anti-CTLA-4 and Anti-PD-1 Checkpoint Blockade. Cell *170*, 1120–1133.e17.

35. Corrales, L., McWhirter, S.M., Dubensky, T.W., Jr., and Gajewski, T.F. (2016). The host STING pathway at the interface of cancer and immunity. J. Clin. Invest. *126*, 2404–2411.

36. Flood, B.A., Higgs, E.F., Li, S., Luke, J.J., and Gajewski, T.F. (2019). STING pathway agonism as a cancer therapeutic. Immunol. Rev. *290*, 24–38.

37. Symons, J.A., Alcamí, A., and Smith, G.L. (1995). Vaccinia virus encodes a soluble type I interferon receptor of novel structure and broad species specificity. Cell *81*, 551–560.

38. Alcamí, A., Symons, J.A., and Smith, G.L. (2000). The vaccinia virus soluble alpha/beta interferon (IFN) receptor binds to the cell surface and protects cells from the antiviral effects of IFN. J. Virol. *74*, 11230–11239.

39. Rubartelli, A., and Lotze, M.T. (2007). Inside, outside, upside down: damage-associated molecular-pattern molecules (DAMPs) and redox. Trends Immunol. *28*, 429–436.

40. Hope, J.L., Stairiker, C.J., Bae, E.A., Otero, D.C., and Bradley, L.M. (2019). Striking a Balance-Cellular and Molecular Drivers of Memory T Cell Development and Responses to Chronic Stimulation. Front. Immunol. *10*, 1595.

41. Hammond, J.M., Oke, P.G., and Coupar, B.E. (1997). A synthetic vaccinia virus promoter with enhanced early and late activity. J. Virol. Methods *66*, 135–138.